Chapter 8
Relaxed Sampling Constraints with Partial Propagations

The sampling constraints for Fresnel propagation are strict. Particularly, the angular-spectrum method is best suited for propagating only short distances. The key problem is wrap-around, caused by aliasing. Several approaches to mitigating these effects have been proposed. Most of these approaches center around spatially attenuating and filtering the optical field. For example, Johnston and Lane describe a technique in which the free-space transfer function is filtered and the grid size is based on the bandwidth of the filter.[41] After this step, they set the sample interval based on avoiding aliasing of the quadratic phase factor just like in Sec. 7.3.2.

Johnston and Lane's choice of spatial-filter bandwidth works, but it is somewhat indirectly related to specific wrap-around effects. This book covers a more direct approach. For fixed D_1, δ_1, D_2, and δ_2, we must satisfy constraints 1, 3, and 4 from Ch. 7. Generally, Δz is fixed, too; it is just a part of the geometry that we wish to simulate. Often, the only free parameter is N, and for large Δz the constraints dictate large N. Sometimes the required N is prohibitively large, like $N > 4096$. Usually the culprit is constraint 4, which is only dependent on the propagation method, not the fixed propagation geometry. If constraint 4 is satisfied, it remains satisfied if we shorten Δz while holding N, δ_1, δ_2, and λ fixed. Consequently, this chapter develops a method of using multiple partial propagations with the angular-spectrum method to significantly relax constraint 4. To illustrate the propagation algorithm, we first begin with two partial propagations in Sec. 8.2 and then generalize to $n - 1$ partial propagations (n planes) in Sec. 8.3.

At first this may sound like a good solution, but multiple partial propagations are mathematically equivalent to a single full propagation. The extra partial propagations just take longer to execute. The key difficulty that we want to mitigate is wrap-around caused by aliasing. The variations in the free-space transfer function, given in Eq. (6.32), become increasingly rapid as Δz increases. Therefore, wrap-around effects creep into the center of the grid from the edge. With partial propagations, we can attenuate the field at the edges of the grid to suppress the wrap-around all along the path. This method allows us to increase the useable range of conditions for our simulation method or reduce the grid size at the cost of executing more

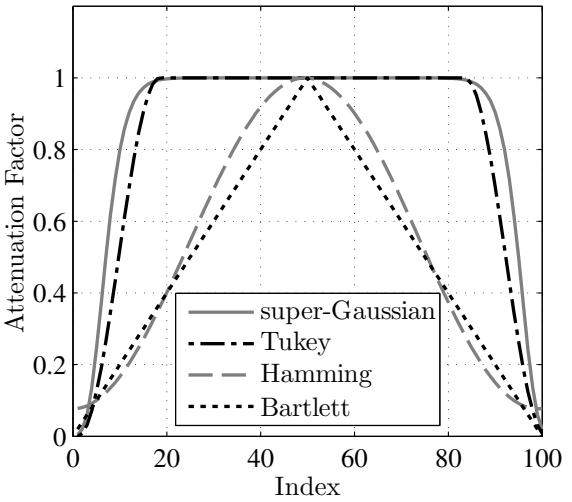

Figure 8.1 Examples of data windows. The super-Gaussian and Tukey windows are appropriate for optical simulations, while the Hamming and Bartlett windows are not. The super-Gaussian shown has $\sigma = 0.45L$ and $n = 16$, while the Tukey window shown has $\alpha = 0.65$.

propagations. In most cases, this shortens the simulation's execution time.

8.1 Absorbing Boundaries

Attenuating the field at the edge has the effect of absorbing energy that is spreading beyond the extent of the grid. The operation is to simply multiply the field by an attenuating factor at each partial-propagation plane. This is similar to the concept of data windowing, but we must be careful not to alter light in the central region of the grid. For this reason, the attenuating factor is very close to unity in the center of the grid and very close to zero at the edge. Common data windows, such as the Hamming and Bartlett windows, are not suited for this purpose. Examples of well suited attenuation factors are the super-Gaussian function defined by

$$g_{sg}(x,y) = \exp\left[-\left(\frac{r}{\sigma}\right)^n\right], \quad n > 2, \tag{8.1}$$

where $n > 2$ and the Tukey (or cosine-taper) window defined by

$$g_{ct}(x,y) = \begin{cases} 1 & r \geq \alpha L/2 \\ \frac{1}{2}\left\{1 + \cos\left[\pi \frac{r/L - \alpha N/2}{(1-\alpha)N/2}\right]\right\} & \alpha N/2 \leq r/L \leq N/2, \end{cases} \tag{8.2}$$

where $0 \leq \alpha \leq 1$ is a parameter that specifies the width of the tapered region. Large α values specify a broad unattenuated region in the center and narrow taper at the edges. These windows are shown in Fig. 8.1.

Absorbing boundaries have been used several times in the literature. For example, Flatté, *et al.* used a super-Gaussian with $n = 8$ to model a plane wave in their

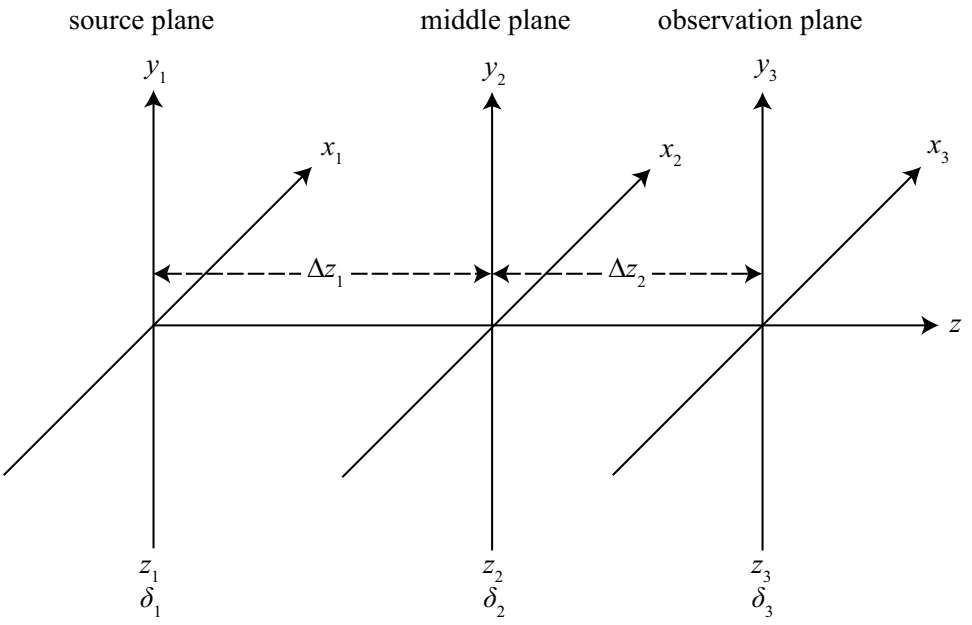

Figure 8.2 Coordinate systems for two partial propagations.

studies of turbulent propagation.[53] Later Rubio adopted the same type of super-Gaussian specifically as an absorbing boundary all along the propagation path.[33] It was used to contain the energy from a diverging spherical wave. The Tukey window was used by Frehlich in his studies of generating atmospheric phase screens.[56]

As an additional example of an absorbing boundary that is not a widely used window, Martin and Flatté used a Gaussian extinction coefficient in their simulations of propagation through atmospheric turbulence.[44] To do so, they added a deterministic imaginary component to their random atmospheric phase screens, thereby multiplying log-amplitude by a Gaussian factor at the edges of the grid. The extinction coefficient in the center of the grid was set to zero so that the field in the center was not attenuated.

8.2 Two Partial Propagations

In this subsection, we simply perform angular-spectrum propagation twice. The first propagation goes from the the source plane to the "middle" plane (somewhere between the source and observation planes, not necessarily half-way), and the second propagation goes from the middle plane to the observation plane. The absorbing boundary is applied in the middle plane after the first propagation. The geometry for two partial propagations is illustrated in Fig. 8.2. The symbols for this subsection are defined in Table 8.1.

Before we get into the simulation equations, we need to determine some mathematical relationships among the symbols in Table 8.1. Figure 8.3 shows the geometry of grid spacings. In the figure, A and B are grid points in the source plane, so

Table 8.1 Definition of symbols for performing two partial propagations.

symbol	meaning
$\mathbf{r}_1 = (x_1, y_1)$	source-plane coordinates
$\mathbf{r}_2 = (x_2, y_2)$	middle-plane coordinates
$\mathbf{r}_3 = (x_3, y_3)$	observation-plane coordinates
δ_1	grid spacing in source plane
δ_2	grid spacing in middle plane
δ_3	grid spacing in observation plane
$\mathbf{f}_1 = (f_{x1}, f_{y1})$	spatial frequency of source plane
$\mathbf{f}_2 = (f_{x2}, f_{y2})$	spatial frequency of middle plane
δ_{f1}	grid spacing in source-plane spatial frequency
δ_{f2}	grid spacing in middle-plane spatial frequency
$z_1 = 0$	location of source plane along the optical axis
z_2	location of middle plane along the optical axis
z_3	location of observation plane along the optical axis
Δz_1	distance between source plane and middle plane
Δz_2	distance between middle plane and observation plane
$\Delta z = \Delta z_1 + \Delta z_2$	distance between source plane and observation plane
$\alpha = \Delta z_1 / \Delta z$	fractional distance of first propagation
m	scaling factor from source plane to observation plane
m_1	scaling factor from source plane to middle plane
m_2	scaling factor from middle plane to observation plane

they are separated by a distance δ_1, consistent with Table 8.1. Points C and D are grid points in the middle plane, so according to Table 8.1, they are separated by a distance δ_2. Finally, E and F are grid points in the observation plane, so they are separated by a distance δ_3. Triangles $\triangle BDH$ and $\triangle BFG$ share a vertex, so they are similar triangles. Therefore, their side lengths are related by

$$\frac{\overline{DH}}{\overline{BH}} = \frac{\overline{FG}}{\overline{BG}}. \tag{8.3}$$

The length of segment $\overline{FG}$ is $(\delta_3 - \delta_1)/2$, and the length of segment $\overline{DH}$ is $(\delta_2 - \delta_1)/2$. The length of segment $\overline{BH}$ is Δz_1, and the length of segment $\overline{BG}$ is $\Delta z = \Delta z_1 + \Delta z_2$. With this knowledge, Eq. (8.3) becomes

$$\frac{\delta_2 - \delta_1}{2\,\Delta z_1} = \frac{\delta_3 - \delta_1}{2\,\Delta z} \tag{8.4}$$

$$\delta_2\,\Delta z - \delta_1\,\Delta z = \delta_3\,\Delta z_1 - \delta_1\,\Delta z_1 \tag{8.5}$$

$$\delta_2 = \delta_1 + \frac{\delta_3\,\Delta z_1 - \delta_1\,\Delta z_1}{\Delta z} \tag{8.6}$$

$$\delta_2 = \delta_1 + \alpha\,\delta_3 - \alpha\,\delta_1 \tag{8.7}$$

$$\delta_2 = (1 - \alpha)\,\delta_1 + \alpha\,\delta_3. \tag{8.8}$$

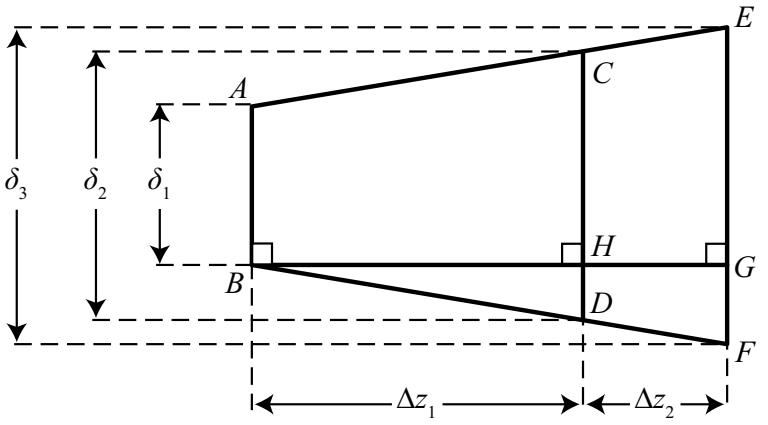

Figure 8.3 Grid spacings for partial propagations.

With these basic relationships among the propagation parameters now known, we can proceed with writing down the equation for performing two successive propagations. When propagating a distance Δz_1 to the middle plane and then propagating a distance Δz_2, the observation-plane field $U(\mathbf{r}_3)$ is given by

$$\begin{aligned} U(\mathbf{r}_3) = {} & \mathcal{Q}\left[\frac{m_2-1}{m_2\,\Delta z_2}, \mathbf{r}_3\right] \mathcal{F}^{-1}\left[\mathbf{f}_2, \frac{\mathbf{r}_3}{m_2}\right] \\ & \times \mathcal{Q}_2\left[-\frac{\Delta z_2}{m_2}, \mathbf{f}_2\right] \mathcal{F}[\mathbf{r}_2, \mathbf{f}_2]\, \mathcal{Q}\left[\frac{1-m_2}{\Delta z_2}, \mathbf{r}_2\right] \frac{1}{m_2} \\ & \times \mathcal{A}[\mathbf{r}_2]\, \mathcal{Q}\left[\frac{m_1-1}{m_1\,\Delta z_1}, \mathbf{r}_2\right] \mathcal{F}^{-1}\left[\mathbf{f}_1, \frac{\mathbf{r}_2}{m_1}\right] \mathcal{Q}_2\left[-\frac{\Delta z_1}{m_1}, \mathbf{f}_1\right] \\ & \times \mathcal{F}[\mathbf{r}_1, \mathbf{f}_1]\, \mathcal{Q}\left[\frac{1-m_1}{\Delta z_1}, \mathbf{r}_1\right] \frac{1}{m_1} \{U(\mathbf{r}_1)\}, \end{aligned} \tag{8.9}$$

where $\mathcal{A}[\mathbf{r}_2]$ is the operator corresponding to the absorbing boundary that is applied to the field in plane 2 (super-Gaussian, Tukey, or similar). The effect of this operator is to multiply the field by a function which reduces the field's amplitude near the edge of the grid.

The quadratic phase factors and the absorbing boundary all commute with each other because they are just multiplicative factors. This may allow us to combine the two middle-plane quadratic phase factors, thus eliminating a step and gaining a little computational efficiency. The product

$$\mathcal{Q}\left[\frac{1-m_2}{\Delta z_2}, \mathbf{r}_2\right] \mathcal{Q}\left[\frac{m_1-1}{m_1\,\Delta z_1}, \mathbf{r}_2\right]$$

can be simplified. To do so, we seek a relationship between the arguments $(1-m_2)/\Delta z_2$ and $(m_1-1)/(m_1\,\Delta z_1)$. Let us revisit Eq. (8.5) and work the factors m_1 and m_2 into the equation

$$\delta_2\,\Delta z - \delta_1\,\Delta z = \delta_3\,\Delta z_1 - \delta_1\,\Delta z_1 \tag{8.10}$$

$$\delta_2 \Delta z_1 + \delta_2 \Delta z_2 - \delta_1 \Delta z_1 - \delta_1 \Delta z_2 = \delta_3 \Delta z_1 - \delta_1 \Delta z_1 \tag{8.11}$$

$$\delta_3 \Delta z_1 - \delta_2 \Delta z_1 = \delta_2 \Delta z_2 - \delta_1 \Delta z_2 \tag{8.12}$$

$$\frac{\delta_3 - \delta_2}{\Delta z_2} = \frac{\delta_2 - \delta_1}{\Delta z_1} \tag{8.13}$$

$$\frac{\delta_3 - \delta_2}{\delta_2 \Delta z_2} = \frac{\delta_2 - \delta_1}{\delta_2 \Delta z_1} \tag{8.14}$$

$$\frac{m_2 - 1}{\Delta z_2} = \frac{m_1 - 1}{m_1 \Delta z_1} \tag{8.15}$$

Therefore, the quadratic phase factors become

$$\mathcal{Q}\left[\frac{1-m_2}{\Delta z_2}, \mathbf{r}_2\right] \mathcal{Q}\left[\frac{m_1 - 1}{m_1 \Delta z_1}, \mathbf{r}_2\right] = \mathcal{Q}\left[-\frac{m_1 - 1}{m_1 \Delta z_1}, \mathbf{r}_2\right] \mathcal{Q}\left[\frac{m_1 - 1}{m_1 \Delta z_1}, \mathbf{r}_2\right] = 1.$$

With this simplification, Eq. (8.9) becomes

$$U(\mathbf{r}_3) = \mathcal{Q}\left[\frac{m_2 - 1}{m_2 \Delta z_2}, \mathbf{r}_3\right] \mathcal{F}^{-1}\left[\mathbf{f}_2, \frac{\mathbf{r}_3}{m_2}\right] \mathcal{Q}_2\left[-\frac{\Delta z_2}{m_2}, \mathbf{f}_2\right] \mathcal{F}[\mathbf{r}_2, \mathbf{f}_2] \frac{1}{m_2}$$
$$\times \mathcal{A}[\mathbf{r}_2] \mathcal{F}^{-1}\left[\mathbf{f}_1, \frac{\mathbf{r}_2}{m_1}\right] \mathcal{Q}_2\left[-\frac{\Delta z_1}{m_1}, \mathbf{f}_1\right] \mathcal{F}[\mathbf{r}_1, \mathbf{f}_1] \mathcal{Q}\left[\frac{1-m_1}{\Delta z_1}, \mathbf{r}_1\right] \frac{1}{m_1} \{U(\mathbf{r}_1)\}. \tag{8.16}$$

This specific result is not implemented in any simulation, but it helps establish a pattern for use with an arbitrary number of partial propagations.

8.3 Arbitrary Number of Partial Propagations

To get a useful result from the previous section, we must generalize it to an arbitrary number of partial propagations. First, let us write the table of propagation and simulation parameters more generally. These parameters are given in Table 8.2 for n propagation planes and $n-1$ partial propagations. As examples, the quantities for the first propagation are given in Table 8.3, and the quantities for the second propagation are given in Table 8.4.

Let us reorder (when possible) and group factors in Eq. (8.16) so that

$$\begin{aligned} U(\mathbf{r}_3) \;= & \mathcal{Q}\left[\frac{m_2 - 1}{m_2 \Delta z_2}, \mathbf{r}_3\right] \left\{ \mathcal{F}^{-1}\left[\mathbf{f}_2, \frac{\mathbf{r}_3}{m_2}\right] \mathcal{Q}_2\left[-\frac{\Delta z_2}{m_2}, \mathbf{f}_2\right] \mathcal{F}[\mathbf{r}_2, \mathbf{f}_2] \frac{1}{m_2} \right\} \\ & \times \left\{ \mathcal{A}[\mathbf{r}_2] \mathcal{F}^{-1}\left[\mathbf{f}_1, \frac{\mathbf{r}_2}{m_1}\right] \mathcal{Q}_2\left[-\frac{\Delta z_1}{m_1}, \mathbf{f}_1\right] \mathcal{F}[\mathbf{r}_1, \mathbf{f}_1] \frac{1}{m_1} \right\} \\ & \times \left\{ \mathcal{Q}\left[\frac{1-m_1}{\Delta z_1}, \mathbf{r}_1\right] U(\mathbf{r}_1) \right\}. \end{aligned} \tag{8.17}$$

Now, it is clear what operations are repeated for each partial propagation, so it is straightforward to generalize this to $n-1$ partial propagations:

$$U(\mathbf{r}_n) = \mathcal{Q}\left[\frac{m_{n-1} - 1}{m_{n-1} \Delta z_{n-1}}, \mathbf{r}_n\right]$$

$$\times \prod_{i=1}^{n-1} \left\{ \mathcal{A}\left[\mathbf{r}_{i+1}\right] \mathcal{F}^{-1} \left[\mathbf{f}_i, \frac{\mathbf{r}_{i+1}}{m_i} \right] \mathcal{Q}_2 \left[-\frac{\Delta z_i}{m_i}, \mathbf{f}_i \right] \mathcal{F}\left[\mathbf{r}_i, \mathbf{f}_i\right] \frac{1}{m_i} \right\}$$
$$\times \left\{ \mathcal{Q} \left[\frac{1-m_1}{\Delta z_1}, \mathbf{r}_1 \right] U\left(\mathbf{r}_1\right) \right\}. \tag{8.18}$$

Listing 8.1 shows code for evaluating the Fresnel diffraction integral in MATLAB using an arbitrary number of partial propagations with the angular-spectrum method. In the listing, the inputs are

Uin : $U\left(\mathbf{r}_1\right)$, the optical field in the source plane $[\left(\mathrm{W/m^2}\right)^{1/2}]$,

wvl : λ, the optical wavelength (m),

delta1 : δ_1, grid spacing in the source plane (m),

deltan : δ_n, grid spacing in the observation plane (m),

z : an array containing the values of z_i for $i = 2, 3, \ldots n$ (m).

The outputs are

xn : x coordinates in the observation plane (m),

yn : y coordinates in the observation plane (m),

Uout : $U\left(\mathbf{r}_n\right)$, optical field values in the observation plane $[\left(\mathrm{W/m^2}\right)^{1/2}]$.

After the sampling is discussed in the next section, an example simulation is presented to illustrate the accuracy of this method.

8.4 Sampling for Multiple Partial Propagations

With an arbitrary number of planes and repeated partial propagations, the sampling constraints must be re-examined. Chapter 7 discusses proper sampling for one complete propagation in detail. It includes a set of four inequalities that must be satisfied when choosing grid spacings and the number of grid points. The first two inequalities are based on the propagation geometry, not the propagation method, so when using multiple partial propagations, they remain unchanged. However, the last two inequalities prevent aliasing of two quadratic phase factors, which depend on grid spacings and propagation distance. The grid spacings and propagation distances can change for every partial propagation, so we need to modify our approach.

Recall that constraint 3 is based on avoiding aliasing of the quadratic phase factor inside the FT of the angular-spectrum method. The same concept applies here. Again we assume a spherical source wavefront with radius R so that the combined phase of the source field and the quadratic phase factor is

$$\phi = \frac{k}{2} \left(\frac{1-m_1}{\Delta z_1} + \frac{1}{R} \right) \left|\mathbf{r}_1\right|^2. \tag{8.19}$$

Table 8.2 Definition of symbols for performing an arbitrary number of partial propagations.

quantity	description
n	number of planes
$n-1$	number of propagations
for the i^{th} propagation	
$\Delta z_i = z_{i+1} - z_i$	propagation distance from plane i to plane $i+1$
$\alpha_i = z_i/\Delta z$	fractional distance from plane 1 to plane $i+1$
$m_i = \delta_{i+1}/\delta_i$	scaling factor from plane i to plane $i+1$
source plane has	
$\mathbf{r}_i = (x_i, y_i)$	coordinates
$\delta_i = (1-\alpha_i)\,\delta_1 + \alpha_i \delta_n$	grid spacing in the i^{th} plane
$\mathbf{f}_i = (f_{xi}, f_{yi})$	spatial-frequency coordinates
$\delta_{fi} = 1/\left(N\delta_i\right)$	grid spacing in spatial-frequency domain
observation plane has	
$\mathbf{r}_{i+1} = (x_{i+1}, y_{i+1})$	coordinates
$\delta_{i+1} = (1-\alpha_{i+1})\,\delta_1 + \alpha_{i+1}\delta_n$	grid spacing

Table 8.3 Symbols for performing the first of an arbitrary number of partial propagations.

symbol	meaning
for the 1st propagation	
$\Delta z_1 = z_2 - z_1$	propagation distance from plane 1 to plane 2
$\alpha_1 = z_1/\Delta z = 0$	fractional distance from plane 1 to plane 1
$\alpha_2 = z_2/\Delta z$	fractional distance from plane 1 to plane 2
$m_1 = \delta_2/\delta_1$	scaling factor from plane 1 to plane 2
source has	
$\mathbf{r}_1 = (x_1, y_1)$	coordinates
δ_1	grid spacing in the 1st plane
$\mathbf{f}_1 = (f_{x1}, f_{y1})$	spatial-frequency coordinates
δ_{f1}	grid spacing in spatial-frequency domain
observation plane has	
$\mathbf{r}_2 = (x_2, y_2)$	coordinates
δ_2	grid spacing

Table 8.4 Symbols for performing the second of an arbitrary number of partial propagations.

symbol	meaning
for the 2nd propagation	
$\Delta z_2 = z_3 - z_2$	propagation distance from plane 2 to plane 3
$\alpha_2 = z_2/\Delta z$	fractional distance from plane 1 to plane 2
$\alpha_3 = z_3/\Delta z$	fractional distance from plane 1 to plane 3
$m_2 = \delta_3/\delta_2$	scaling factor from plane 2 to plane 3
source has	
$\mathbf{r}_2 = (x_2, y_2)$	coordinates
δ_2	grid spacing in the 2nd plane
$\mathbf{f}_2 = (f_{x2}, f_{y2})$	spatial-frequency coordinates
δ_{f2}	grid spacing in spatial-frequency domain
observation plane has	
$\mathbf{r}_3 = (x_3, y_3)$	coordinates
δ_3	grid spacing

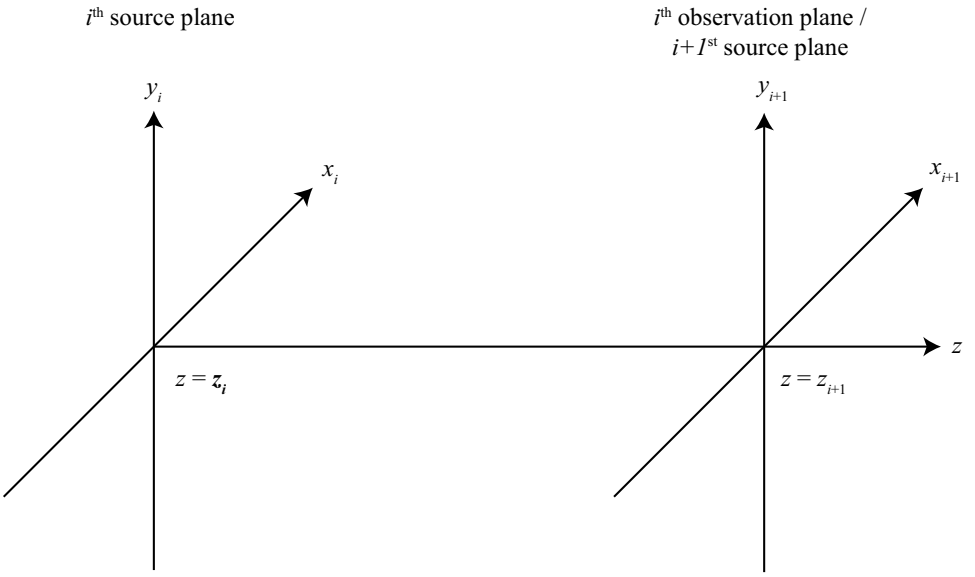

Figure 8.4 Coordinate systems for a single partial propagation.

Listing 8.1 Code for evaluating the Fresnel diffraction integral in MATLAB using an arbitrary number of partial propagations with the angular-spectrum method.

```
function [xn yn Uout] = ang_spec_multi_prop_vac ...
    (Uin, wvl, delta1, deltan, z)
% function [xn yn Uout] = ang_spec_multi_prop_vac ...
%     (Uin, wvl, delta1, deltan, z)

    N = size(Uin, 1);   % number of grid points
    [nx ny] = meshgrid((-N/2 : 1 : N/2 - 1));
    k = 2*pi/wvl;    % optical wavevector
    % super-Gaussian absorbing boundary
    nsq = nx.^2 + ny.^2;
    w = 0.47*N;
    sg = exp(-nsq.^8/w^16); clear('nsq', 'w');

    z = [0 z];  % propagation plane locations
    n = length(z);
    % propagation distances
    Delta_z = z(2:n) - z(1:n-1);
    % grid spacings
    alpha = z / z(n);
    delta = (1-alpha) * delta1 + alpha * deltan;
    m = delta(2:n) ./ delta(1:n-1);
    x1 = nx * delta(1);
    y1 = ny * delta(1);
    r1sq = x1.^2 + y1.^2;

    Q1 = exp(i*k/2*(1-m(1))/Delta_z(1)*r1sq);
    Uin = Uin .* Q1;
    for idx = 1 : n-1
        % spatial frequencies (of i^th plane)
        deltaf = 1 / (N*delta(idx));
        fX = nx * deltaf;
        fY = ny * deltaf;
        fsq = fX.^2 + fY.^2;
        Z = Delta_z(idx);   % propagation distance
        % quadratic phase factor
        Q2 = exp(-i*pi^2*2*Z/m(idx)/k*fsq);
        % compute the propagated field
        Uin = sg .* ift2(Q2 ...
            .* ft2(Uin / m(idx), delta(idx)), deltaf);
    end
    % observation-plane coordinates
    xn = nx * delta(n);
    yn = ny * delta(n);
    rnsq = xn.^2 + yn.^2;
    Q3 = exp(i*k/2*(m(n-1)-1)/(m(n-1)*Z)*rnsq);
    Uout = Q3 .* Uin;
```

At first, this constraint looks confusing because it depends on Δz_1, and we cannot determine Δz_1 until the rest of the sampling analysis is complete! Nonetheless, we carry on with the analysis. It proceeds just like in Eqs. (7.48)–(7.53) to yield

$$\left(1+\frac{\Delta z_1}{R}\right)\delta_1 - \frac{\lambda\Delta z_1}{D_1} \leq \delta_2 \leq \left(1+\frac{\Delta z_1}{R}\right)\delta_1 + \frac{\lambda\Delta z_1}{D_1}. \tag{8.20}$$

Now, we substitute in for δ_2 and Δz_1 to get

$$\left(1+\frac{\alpha_2\Delta z}{R}\right)\delta_1 - \frac{\lambda\alpha_2\Delta z}{D_1} \leq (1-\alpha_2)\,\delta_1 + \alpha_2\delta_n \leq \left(1+\frac{\alpha_2\Delta z}{R}\right)\delta_1 + \frac{\lambda\alpha_2\Delta z}{D_1}. \tag{8.21}$$

After multiplying everything out and eliminating common terms, we are left with

$$\left(1+\frac{\Delta z}{R}\right)\delta_1 - \frac{\lambda\Delta z}{D_1} \leq \delta_n \leq \left(1+\frac{\Delta z}{R}\right)\delta_1 + \frac{\lambda\Delta z}{D_1}. \tag{8.22}$$

This is identical to Eq. (7.53), which has no dependence on quantities related to partial-propagation planes, like δ_2 and Δz_1!

Now, constraint 4 is the only one left to modify, and we must find a way to relate it to n. Hopefully, it is related in such a way that n partial propagations relaxes this constraint. For the the i^{th} partial propagation, it is given by

$$N \geq \frac{\lambda\Delta z_i}{\delta_i\delta_{i+1}}. \tag{8.23}$$

This makes a very complicated parameter space. To simplify, we can write all δ_i in terms of δ_1 and δ_n. However, that just exchanges δ_i for α_i, which depends on z_i. There is just no way to reduce the dimensions of the parameter space for this constraint. Rather than trying to satisfy all n constraints implied by Eq. (8.23), we only need to satisfy the case for which the right-hand side is a maximum. However, that requires prior knowledge of all the Δz_i and δ_i, which is what we are trying to determine!

Obviously, a new approach is necessary. Let us write down the inequalities again and regroup

1. $\delta_n \leq \frac{\lambda\Delta z - D_2\delta_1}{D_1}$,
2. $N \geq \frac{D_1}{2\delta_1} + \frac{D_2}{2\delta_n} + \frac{\lambda\Delta z}{2\delta_1\delta_n}$,
3. $\left(1+\frac{\Delta z}{R}\right)\delta_1 - \frac{\lambda\Delta z}{D_1} \leq \delta_n \leq \left(1+\frac{\Delta z}{R}\right)\delta_1 + \frac{\lambda\Delta z}{D_1}$,
4. $N \geq \frac{\lambda\Delta z_i}{\delta_i\delta_{i+1}}$.

Examining the inequalities, we can see that it is possible to use the first three inequalities to choose values of N, δ_1, and δ_n. Then, we can find a way to satisfy the fourth constraint.

Depending on whether we are using expanding or contracting propagation grids, either δ_1 or δ_n is smaller than all other δ_i. For a given value of Δz_i, picking the smaller of δ_1 and δ_n to replace δ_i and δ_{i+1} in the fourth inequality gives us a single constraint that N must satisfy. However, N is already chosen using the first two constraints, and the limit on Δz_i remains unknown, so we must rewrite the inequality as a constraint on Δz_i so that

$$\Delta z_i \leq \frac{\min\left(\delta_1, \delta_n\right)^2 N}{\lambda}. \tag{8.24}$$

The right-hand side is the maximum possible partial-propagation distance Δz_{max} that can be used. Therefore, we must use at least $n = \text{ceil}\left(\Delta z / \Delta z_{max}\right) + 1$ partial propagations (where ceil is the "ceiling" function; it produces the smallest integer value that is greater than or equal to its argument).

Finally, with this new view of the fourth inequality, the method of choosing propagation-grid parameters is clear:

1. First, pick N, δ_1, and δ_n based on the first two inequalities.

2. Then, use a slightly adjusted version of the fourth inequality [Eq. (8.24)] to determine the maximum partial-propagation distance and the minimum number of partial propagations $n - 1$ together.

3. One can always use more partial propagations; shorter partial-propagation distances still satisfy the fourth inequality.

We close this chapter with an example of using this method to achieve accurate results within the observation-plane region of interest. In this example, we want to simulate propagation of a uniform-amplitude plane wave ($R = \infty$) departing a square aperture in the source plane. The aperture has $D_1 = 2$ mm across each side. The optical wavelength is $\lambda = 1\,\mu$m, and the sensor is in the observation plane located $\Delta z = 2$ m from the source plane. Figure 8.5 shows a contour plot of constraint 2 with a plot of constraint 1 overlayed. Often, it is helpful to have a certain number of grid points across the source aperture and the observation-plane region of interest. For this example, we choose to have at least 30 grid points across D_1 and D_2. This choice gives $\delta_1 \leq 66.7\,\mu$m and $\delta_n \leq 133\,\mu$m. According to the contour plot, at least $N = 2^7 = 128$ grid points are required. To conclude the sampling analysis, we apply constraint 4 with $\delta_1 = 66.7\,\mu$m, $\delta_n = 133\,\mu$m, and $N = 128$. This gives

$$\Delta z_{max} = \frac{\min\left(\delta_1, \delta_n\right)^2 N}{\lambda} = \frac{\left(66.7\,\mu\text{m}\right)^2\ 128}{1\,\mu\text{m}} = 0.567\,\text{m}. \tag{8.25}$$

Then, we need to perform at least $n = \text{ceil}\left(2\,\text{m}/0.567\,\text{m}\right) + 1 = 5$ partial propagations. Listing 8.2 gives the MATLAB code used to simulate the propagation for this

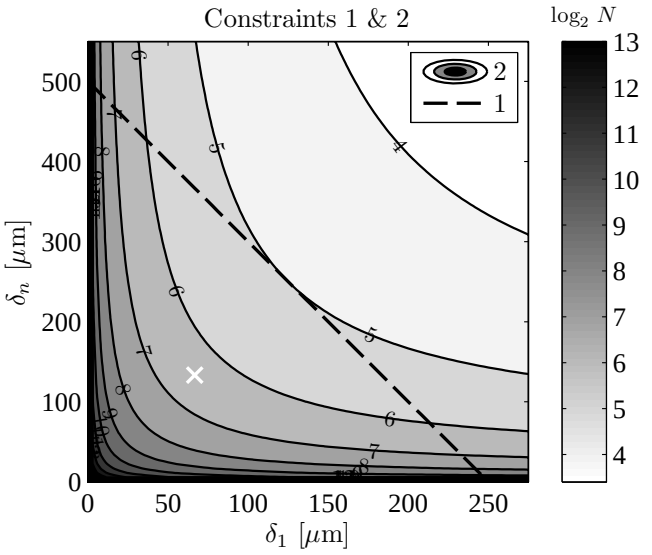

Figure 8.5 Analysis of sampling constraints. The white x marks grid spacings that correspond to 30 grid points across the source- and observation-plane apertures.

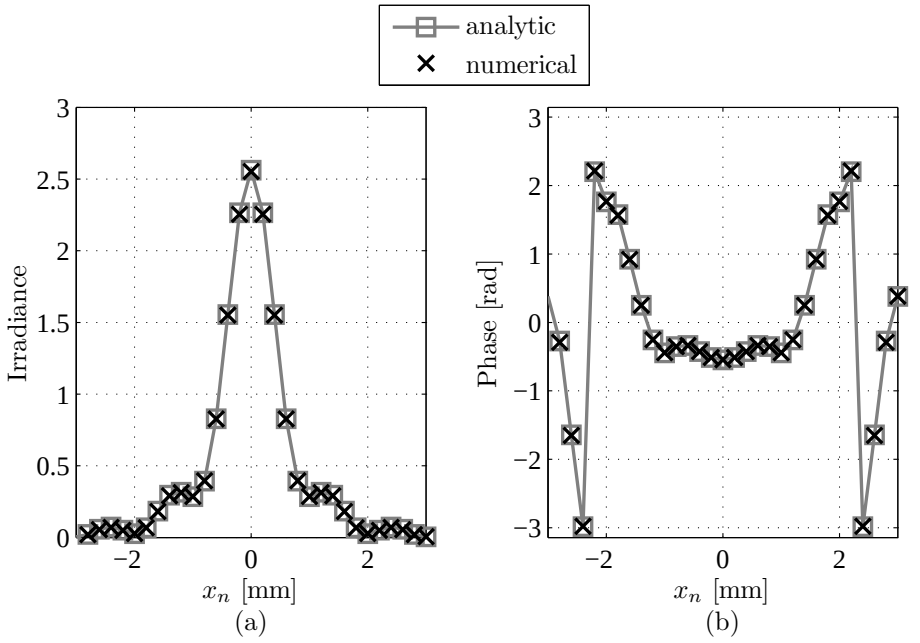

Figure 8.6 Simulated irradiance and phase in the observation-plane region of interest.

example. Figure 8.6 shows the simulated irradiance and phase in the observation-plane region of interest. As usual, the simulation result matches the theoretical expectation closely in the observation-plane region of interest.

Listing 8.2 Example of evaluating the Fresnel diffraction integral in MATLAB using the angular-spectrum method with several partial propagations.

```
% example_square_prop_ang_spec_multi.m

D1 = 2e-3;   % diameter of the source aperture [m]
D2 = 6e-3;   % diameter of the observation aperture [m]
wvl = 1e-6;  % optical wavelength [m]
k = 2*pi / wvl; % optical wavenumber [rad/m]
z = 2;     % propagation distance [m]
delta1 = D1/30; % source-plane grid spacing [m]
deltan = D2/30; % observation-plane grid spacing [m]
N = 128;        % number of grid points
n = 5;          % number of partial propagations
% switch from total distance to individual distances
z = (1:n) * z / n;
% source-plane coordinates
[x1 y1] = meshgrid((-N/2 : N/2-1) * delta1);
ap = rect(x1/D1) .* rect(y1/D1);    % source aperture
[x2 y2 Uout] = ...
    ang_spec_multi_prop_vac(ap, wvl, delta1, deltan, z);

% analytic result for y2=0 slice
Dz = z(end); % switch back to total distance
Uout_an ...
    = fresnel_prop_square_ap(x2(N/2+1,:), 0, D1, wvl, Dz);
```

8.5 Problems

1. Consider the signal

$$g(x) = \exp\left(i\pi a^2 x^2\right) \tag{8.26}$$

with $a = 4$ sampled on a grid with $N = 128$ points and $L = 4$ m total grid size. Compute both the analytic and discrete FT of this signal. Next, pre-multiply the signal by a super-Gaussian absorbing boundary function with $n = 16$ and $\sigma = 0.25L$ and compute the DFT again. Plot the imaginary and real parts of the two DFT results (with and without the absorbing boundary) and compare against the analytic FT.

2. Fill in the missing steps between Eqs. (8.20) and (8.22) to show that constraint 3 is identical for any number of partial propagations.

3. Show the sampling diagram for a point source with wavelength 1 μm propagating 100 km to a telescope with a 2-m-diameter aperture. How does this compare to the case when there is only one propagation?

4. Simulate propagation of a uniform-amplitude plane wave from an annular aperture to a target plane with the source beam focused onto the target. Let the annular aperture have an outer diameter of 1.5 m and an inner diameter of 0.5 m. Let the optical wavelength be 1.3 μm. Place the target in the observation plane 100 km away from the source plane.

   (a) Show a detailed sampling analysis similar to that shown in Fig. 8.5. Be sure to describe your analysis of determining the number of partial propagations to use.

   (b) After completing the simulation, show plots of the $y_n = 0$ slice of the observation-plane irradiance and phase. Include the analytic and simulation results on the same plot.